

Nuclear Gamma-Rays from Low Energy Proton Bombardment of Sodium, Magnesium, and Aluminum

HARVEY CASSON*

Department of Physics and Institute for Nuclear Studies, University of Chicago, Chicago, Illinois

(Received September 22, 1952)

Gamma-rays produced by the resonance capture of 200–415-keV protons in sodium, magnesium, and aluminum have been investigated with a single crystal NaI(Tl) scintillation spectrometer. Excited states in Mg^{24} , Al^{25} , Al^{27} , and Si^{28} with energies above the ground state of 12 MeV, 2.5 MeV, 8.6 MeV, and 12 MeV, respectively, were found to decay by cascade gamma-emission. Direct transitions to the ground state of Mg^{24} , Al^{27} , and Si^{28} were not observed. Observed pulse-height distributions, location of observed peaks, identifiable gamma-rays and their relative intensities are given. Decay schemes are proposed to account for the observed gamma-rays of Al^{27} , Si^{28} , and Al^{25} . They are found to involve energy levels which are in general agreement with levels found in (d,n) and (p,p) scattering experiments; in the case of Al^{25} , with levels found in the mirror nucleus Mg^{25} . An estimate is made of the absolute proton capture probability in the targets used.

I. INTRODUCTION

TANGEN,¹ using G-M counter detection, has investigated a number of (p,γ) resonances among the lighter elements for proton energies up to 500 keV but, using absorption techniques, was only able to report the mean gamma-ray energies. Since the mean energies have frequently been considerably lower than the calculated excitation energies, this suggests the likelihood of cascade emission. In the present work the energies and relative intensities of the gamma-rays arising from several such (p,γ) resonances were measured, using a sodium iodide (single crystal) scintillation spectrometer. In simple cases, at least, such an energy study might be expected to indicate the most probable modes of decay to the ground state of the nucleus resulting from the proton capture.

The materials selected for proton bombardment were sodium, magnesium, and aluminum, each of which exhibits several sharp but weak (p,γ) resonances within the range of our proton accelerator.

II. SOURCE OF THE BOMBARDING PROTONS

Protons in the energy range from 200–400 keV were obtained from the new Cockcroft-Walton accelerator, or "kevatron" of the Institute for Nuclear Studies at the University of Chicago.

The protons were extracted from a capillary type ion source,² accelerated down a quartz tube containing 15 accelerating sections, and were then magnetically deflected through 15° into the target chamber. Fine adjustment of the position of the beam on the target was accomplished by a pair of electrostatic deflection plates (horizontal and vertical) located just before the magnet.

The high voltage through which the ions were accelerated was determined by measuring the current

passing to ground through a 10^{10} -ohm resistor stack made up of 1000 10-megohm resistors in series.

In frequent practice, the voltage scale was checked by excitation of the gamma-rays from the well-known fluorine reaction: $F^{19}(p;\alpha,\gamma)O^{16}$, which is sharply resonant at a proton energy of 340.4 keV.²

III. TARGET CHAMBER

Owing to the very low yield of γ -rays from the resonances under investigation, the target chamber with which most of the measurements were made was designed to have as small as possible a distance between the target and the detector (see Fig. 1). The target could be preheated to drive off any oil vapors which would be carbonized when struck by the beam. The end of the chamber had attached to it a cooling coil which kept it near room temperature. This allowed the gamma-detector to be moved up to within 3.5 mm of the target surface. The target material was either evaporated (in vacuum) or fused onto pure copper disks, 1 inch in diameter and $\frac{3}{32}$ inch thick. These target disks were dropped into position in the center of the heater assembly and were held in place by means of a split ring of spring wire which slipped into a groove and could easily be removed with forceps.

The target chamber as a whole was insulated from ground and used as a Faraday cup to measure the beam current hitting the target, and electrically biased diaphragms were used (see Fig. 1) to prevent error in the beam current readings from secondary electrons.

IV. BEAM CURRENT INTEGRATOR

The beam current integrator has been in the laboratory in satisfactory operation for several years. It involves a feedback circuit which prevents the input lead from rising very much above ground potential, thus minimizing spurious leakage currents. It was started simultaneously with the gamma-ray count and after a preset number of microcoulombs of protons hitting the target, the count was automatically stopped. The integrator could be set for 250, 500, 1250, or 2500

* Now at Argonne National Laboratory, P. O. Box 299, Lemont, Illinois.

¹ R. Tangen, "Experimental Investigations of Proton Capture Processes in Light Elements," Kgl. Norske Videnskab. Selskabs, Skrifter, No. 1 (1946).

² A. H. Morrish, Phys. Rev. 76, 1651 (1949).

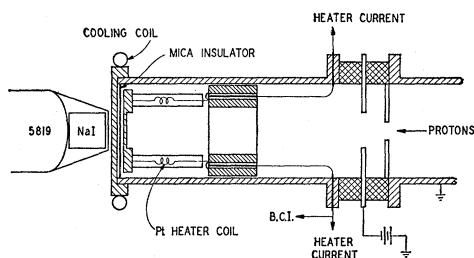


Fig. 1. Target chamber, designed for heating of target, and close proximity of target and sodium iodide crystal.

microcoulombs. Proton beam currents between 6 and 12 microamperes were ordinarily used.

V. THE SCINTILLATION SPECTROMETER

The scintillating crystals used in this work were 1-in. cubes of NaI(Tl).³ The surfaces of the crystal were cut parallel to the cleavage planes. Because of the hygroscopic property of sodium iodide, the crystals were stored in dried mineral oil when not in use, and a thin layer of either mineral oil or vacuum grease was kept over their surfaces under all other circumstances.

The crystals, with their surfaces cleaned,⁴ were placed in optical contact with the entrance window of the photomultiplier tube (RCA 5819) and covered with a reflector of shiny aluminum foil.

Two photomultiplier tubes were used at various times during the research. They were selected from about six tubes of the same type. The pulse output of the photomultiplier went to a pre-amplifier of the type described by Allen;⁵ the pre-amplifier output went to a Los Alamos Model 500 linear amplifier, as described by Elmore and Sands.⁶

A single-channel differential discriminator (Fig. 2) was constructed for the analysis of pulse heights. It consisted of two Schmidt⁷ discriminator circuits, two univibrator circuits,⁷ and one anticoincidence gate circuit, operated by a regulated power supply. The common cathodes of the two Schmidt circuits were kept at a fixed difference in bias. (This determined the channel width.) The input grids were tied together to the variable arm of a ten-turn 0.1 percent linearity helipot whose dial setting determined the voltage of the base of the channel. The univibrator which followed the lower discriminator was used as a time-delay pulse shaper; the univibrator following the upper one provided a rectangular gating pulse. Only when the lower,

but not the upper, of the two discriminator circuits was triggered would a pulse arrive at the output.

The time delay was about 5 microseconds; the gating pulse had a width of about 10 microseconds. The rise time of the pulses from the amplifier was about 1 microsecond. The circuit was fast enough to handle adequately the counting rates ordinarily observed in our work.

The output of the single-channel discriminator went to a Los Alamos Model 200 scale of 64,⁸ whose input was either shorted or open as determined by the relay circuit associated with the beam current integrator.

VI. INTERPRETATION OF PULSE-HEIGHT DISTRIBUTIONS

It has been shown experimentally⁹ that when a clear NaI(Tl) crystal (that is, a sodium iodide crystal grown with a few percent of thallium iodide added as an impurity) is bombarded with γ -radiation, the light output is strictly proportional to the energy absorbed, over a large range of energies.

Whereas alphas or betas slow down directly, a photon of energy E_0 must first produce electrons in motion by (1) photoelectric effect, (2) Compton effect, (3) pair production in the crystal. Although (1) leaves an atom with a vacancy in the K or L shell, the resultant x-radiation is usually reabsorbed in the crystal so that the light pulse corresponds to energy E_0 . (2) produces a continuous distribution of electron energies up to a maximum which is less than E_0 and may be expressed, by direct calculation from the Compton equation,¹⁰ in the following form:

$$(E_c)_{\max} = \frac{1}{1 + mc^2/2E_0} \times E_0 = E_0 \frac{mc^2/2}{1 + mc^2/2E_0}. \quad (1)$$

This point is referred to as the Compton edge.

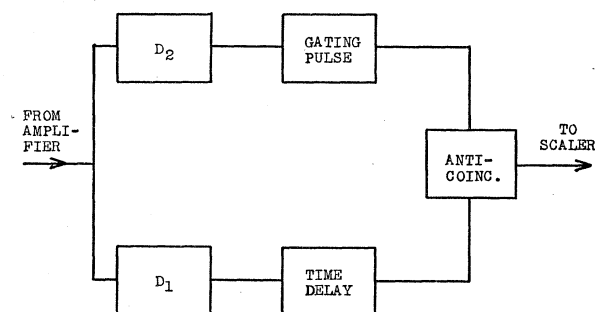


Fig. 2. Block diagram of the single-channel differential discriminator.

³ Harshaw Chemical Company, Cleveland, Ohio.

⁴ Fresh, transparent surfaces on the crystals were obtained by placing them successively in baths of (a) *n*-butyl alcohol, (b) *n*-butyl alcohol mixed with xylene, and (c) xylene, following a technique privately communicated by W. Bernstein of the Brookhaven National Laboratory.

⁵ J. S. Allen, *Rev. Sci. Instr.* **18**, 743 (1947).

⁶ W. C. Elmore and Matthew L. Sands, *Electronics: Experimental Techniques* (McGraw-Hill Book Company, Inc., New York, 1949), p. 167 and Sec. 7.2.

⁷ Reference 6, pp. 99 ff, Chap. IV, 87 ff, pp. 120-123.

⁸ Reference 6, p. 218.

⁹ See, for example, R. Hofstadter and J. A. McIntyre, *Nucleonics* **7**, 32 (1950).

¹⁰ See, for example, W. Heitler, *Quantum Theory of Radiation* (Oxford University Press, London, 1947), second edition, p. 146. The maximum electron energy is obtained for backscattering of the radiation. Putting $\cos\theta = -1$ and evaluating the change in quantum energy gives the result stated.

For $E_0 \gg mc^2$, Eq. (1) shows that the Compton edge occurs at approximately $E_0 - \frac{1}{2}mc^2$. Evaluation of the Klein-Nishina formula to obtain the energy distribution of the Compton electrons gives an almost flat distribution which rises to a sharp maximum at the Compton edge and is zero above the edge. Experimentally, we find this maximum to lie between $E_0 - mc^2$ and $E_0 - \frac{1}{2}mc^2$.

In case (3), an electron and positron are created in the crystal with kinetic energies initially adding up to $E_0 - 2mc^2$. They are slowed down to zero energy and the positron is annihilated, yielding 2 quanta of energy mc^2 . If both quanta are absorbed in the crystal, the total light pulse corresponds to E_0 ; if one escapes, $E_0 - mc^2$; and if both escape, $E_0 - 2mc^2$. For the case of pairs produced close enough to a surface of the crystal to allow one or both of the electrons to leave the crystal before being completely stopped, a continuous distribution of pulses less than E_0 is obtained.

The resultant pulse-height distribution due to an incident gamma-quantum of energy $E_0 \gg mc^2$ may be described as follows. Three peaks may be observed: P_3 at pulse height E_0 , owing to a superposition of all processes in which the full gamma-ray energy is absorbed in the crystal (i.e., all secondary radiations are absorbed); P_2 at pulse height approximately $E_0 - mc^2$, arising from pair production with one of the annihilation quanta captured, superimposed on the peak of the Compton distribution; and P_1 at pulse height $E_0 - 2mc^2$ from pair production with both annihilation quanta escaping. The observed *continuous* distribution of lower energy pulses is mainly due to a superposition of the Compton distribution and the distribution due to pair, photo, and Compton electrons which are not completely stopped in the crystal.

Since the above processes have different energy dependence, the appearance of a distribution may be expected to change considerably with the energy of the incident gamma.

For a 1-inch cubic NaI crystal, and gamma-energy

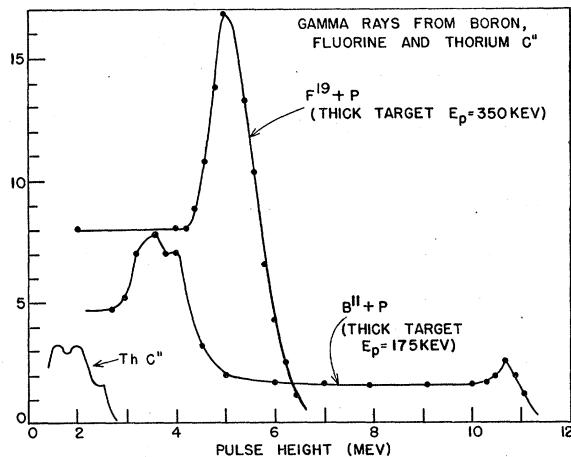


Fig. 3. Spectra of gamma-rays of various energies used in calibrating the spectrometer.

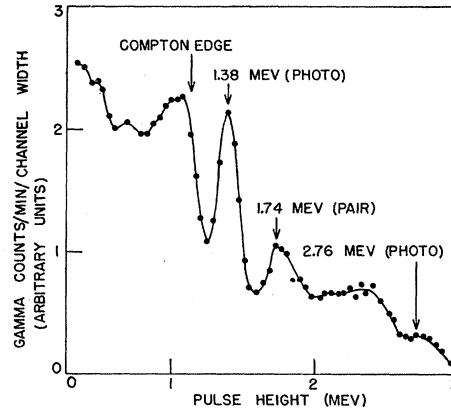


Fig. 4. Gamma-ray spectrum from a Na^{24} source. The distributions due to the 1.38-Mev and 2.76-Mev cascade gamma-rays are superimposed.

E_0 less than 0.5 Mev, the peak E_0 tends to predominate due to large photoeffect and large probability that any secondary radiations will be absorbed in the crystal. Between 0.5 Mev and about 2 Mev one observes mainly the Compton peak and the photopeak. Between 2 and 4 Mev, one observes $E_0 - 2mc^2$, $E_0 - mc^2$, with a much smaller peak at E_0 . Above 4 Mev the peak at E_0 was not observed. Instead, $E_0 - mc^2$ decreases relative to $E_0 - 2mc^2$ (because of the decrease in the Compton cross section relative to the cross section for pair production), and the latter peak predominates. At some energy above 4 Mev, depending on the resolution of the spectrometer, the smaller peak $E_0 - mc^2$ ceases to be resolved from the larger peak $E_0 - 2mc^2$, and as a result only one peak is seen.

For gamma-rays above 6 Mev (and at least up to 11.5 Mev), the observed distribution was especially simple in form. It consisted of a long flat portion with the peak at $E_0 - 2mc^2$ superimposed.

Figures 3 and 4 show the pulse-height distributions due to gamma-rays of various energies.

Where more than one gamma-ray is present, the interpretation of the peaks may be difficult. This is especially true in the region 2 to 4 Mev since all three of the peaks may be observable.

VII. CALIBRATION AND PERFORMANCE OF THE SCINTILLATION SPECTROMETER

The response of the scintillation spectrometer was calibrated using the following known gamma-ray sources:

Na^{22} and Na^{24}	Hg^{203}
$\text{B}^{11}(p, \gamma)\text{C}^{12}$	Hf^{181}
$\text{F}^{19}(p; \alpha, \gamma)\text{O}^{16}$	Se^{75}

Since the amplifier saturated above 90 volts, and the discriminator did not operate satisfactorily below 10 volts, the range of pulse heights which could be reliably analyzed at a given gain setting of the analyzer was somewhat restricted. In order to cover the gamma-ray

TABLE I. Gamma-ray absorption coefficients.

E_γ (Mev)	Sodium iodide				Copper Total absorption coeff. (cm^{-1})
	Compton absorption coeff. (cm^{-1})	Pair absorption coeff. (cm^{-1})	Photo absorption coeff. (cm^{-1})	Total absorption coeff. (cm^{-1})	
0.5	0.268	...	0.059	0.327	0.72
1.0	0.196	...	0.011	0.207	0.52
2.0	0.136	0.008	0.004	0.148	0.36
3.0	0.106	0.022	0.002	0.130	0.32
4.0	0.086	0.035	0.002	0.123	0.30
5.0	0.074	0.048	0.001	0.123	0.28
6.0	0.066	0.059	0.001	0.126	0.27
7.0	0.060	0.068	0.001	0.129	0.27
8.0	0.056	0.077	...	0.133	0.27
9.0	0.051	0.085	...	0.136	0.27
10.0	0.047	0.092	...	0.139	0.27
11.0	0.044	0.100	...	0.144	0.27
12.0	0.041	0.107	...	0.148	0.27

energy range from 0.5 to 12 Mev, the range was divided up into several parts each of which was separately calibrated. In the low energy range, the 0.51-Mev and 1.28-Mev gammas of Na^{22} were used; in the high energy range, the Na^{22} 1.28 Mev and fluorine 6.13-Mev gammas were used for the calibration. The ranges were selected by changing the amplifier gain. The channel width most frequently used was about 2 volts, although a 5 volt channel was used when intensities were very low. The results of the calibration confirmed the conclusions of previous investigators concerning the linearity of the pulse height *versus* energy release relation.

The resolution of the spectrometer is defined as the full width at half-maximum of the photopeak of a low energy gamma ($E_\gamma < 3$ Mev, where the photopeak is visible) and is expressed as a percentage of the pulse height at the peak. The best resolution obtained was about 12 percent at 1.28 Mev and 17 percent at 0.5 Mev. At 6 Mev, the peaks at $E - 2mc^2$ and $E - mc^2$ are unresolved giving a single peak. If the resolution for this case is defined as the width of the peak considering the *plateau* to be the zero line, then a value of about 6 percent was obtained. Using the full height of the peak, the width at half-maximum was about 17 percent.

It is believed that by finding a better photomultiplier tube, the resolution could have been improved by about a factor of 2, which would bring it close to the best values attained by other investigators.

VIII. CALCULATION OF INTENSITIES AND YIELDS

The total area under the distribution curve due to a monochromatic beam of γ -rays should be equal to the number of primary gammas which have been absorbed by the crystal. (Secondary absorption and resolution factors would ordinarily affect the location of pulses in the distribution, and hence its shape, but should not change their total number.) The assumption made here is that each time a gamma is absorbed and a light pulse is produced, there are enough photons in the light pulse to assure a probability of unity that the detector will

register the pulse. Only for very low energy pulses (say, pulses corresponding to less than 50 kev of gamma-ray energy) might this assumption be invalid. Since we are concerned at present with gammas of energy greater than 500 kev and extrapolate to zero the observed higher energy part of the pulse-height distribution, such a low energy "cutoff" would not affect the results.

This extrapolated area under the distribution curve owing to a given gamma-ray, we call the "extrapolated yield." The observed pulse-height distributions generally involved a number of gamma-rays. The plateau level due to the highest energy gamma was determined first, either by direct observation when possible, or else by estimation of the expected level in terms of the height of the pair peak. The extrapolated yield was then determined by extending this plateau to zero and calculating the area under this distribution. The plateau of this gamma was assumed to be the zero line of the next lower gamma-ray, and in like manner, the extrapolated yields of this, and successive lower gamma-rays were determined. For γ -rays below 3 Mev, the extrapolation was performed by comparison with known distributions (Na^{24} , Na^{22} , ThC'' , etc.).

In certain cases where a number of peaks were so close to each other that identification of the gamma-rays involved was not certain or else the height of a peak could not be established because of poor statistics, the extrapolated yield for the *sum* of the gamma-rays involved was determined.

In order to be able to compare the various gamma-rays from the point of view of their relative frequency of production in the (p, γ) reactions, it was necessary to know the variation with energy of the total absorption coefficients (photoelectric+Compton+pair) of the gammas in sodium iodide. On the basis of data given in Heitler¹¹ this was calculated; the results are given in Table I.

Since there was about $\frac{1}{8}$ inch of copper between the target surface and the detector, Heitler's values of the total absorption coefficients in copper are also included in Table I. The attenuation of the beam due to the presence of this material (about 15 percent for most of the gamma-rays observed) did not seriously distort the components of the pulse-height distribution, and it should be remembered that calibration of the spectrometer was carried out with the same target and crystal geometry which was later used in investigating the new gamma-rays.

The "relative intensity" of an observed gamma-ray was obtained from the *extrapolated yield* by converting the latter to the extrapolated yield which would have been obtained from a hypothetical gamma of energy 6 Mev and having the same absolute intensity. Both the relative efficiency for absorption in sodium iodide and the relative transmission through the copper were con-

¹¹ Reference 10, Chaps. III, IV, and V.

sidered. Taking these two factors into account mathematically, we may write for the relative intensity

$$I_{\gamma} = \frac{1 - \exp[-\tau_{\text{NaI}}(\delta)\bar{x}]}{1 - \exp[-\tau_{\text{NaI}}(\gamma)\bar{x}]} \times \frac{\exp[-\tau_{\text{Cu}}(\gamma)\bar{y}]}{\exp[-\tau_{\text{Cu}}(\delta)\bar{y}]} \times Y_{\text{ext}}, \quad (2)$$

where τ_{NaI} and τ_{Cu} are the linear absorption coefficients taken from Table I, \bar{x} is the effective thickness of the crystal, \bar{y} the effective thickness of copper, and Y_{ext} is the extrapolated yield.

It should be emphasized that the above definition of "relative intensity" refers to the *number* of gamma-quanta absorbed by the crystal, rather than the number of gamma-quanta multiplied by their energy.

Between 2 and 10 Mev, the relative intensity turns out to be numerically almost the same as the extrapolated yield (within 20 percent). In this region of energies, the exponentials in Eq. (2) may be expanded in series. The first-order approximation, which gave sufficient accuracy, involves merely the ratio of the absorption coefficients $\tau(\gamma)$ and $\tau(\delta)$ in sodium iodide.

In view of the difficulties involved in obtaining extrapolated yields from a complex distribution to an accuracy of much better than 50 percent (uncertainty in extrapolation, decrease in effective target thickness during the course of a run, statistics, etc.), the labor of substitution into Eq. (2) was not warranted for most of the observed gamma-rays.

The analysis of 0.5-Mev radiation must be considered as a special case. The absorption of high energy gammas due to the pair production cross section in the copper resulted in the emanation of annihilation quanta of energy 0.51 Mev from the copper. The excitation of positron-emitting states of short half-life would also produce annihilation radiation (a long half-life would enable this radiation to be detected in the background runs).

Before one can make any claims about the existence of nuclear 0.5-Mev gamma-rays it is necessary to compare the observed intensity of radiation with the total estimated annihilation intensity. A significant difference between the two would then be attributable to nuclear radiation.

For the purpose of estimating absolute gamma-ray yields, a calculation was made of the effective geometry of a cylindrical crystal relative to a point source located along its axis. The assumption was made that the attenuation of the gamma-ray beam on passing through the crystal was negligible.

Straightforward integration gave the following expression for the number Y of gammas absorbed per unit time for a point source of strength S :

$$Y = \frac{S\tau a}{4} \left\{ \frac{x+L}{a} \ln \left[1 + \frac{a^2}{(x+L)^2} \right] - \frac{x}{a} \ln \left(1 + \frac{a^2}{x^2} \right) + 2 \left[\tan^{-1} \frac{x+L}{a} - \tan^{-1} \frac{x}{a} \right] \right\}, \quad (3)$$

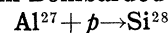
where τ is the gamma-absorption coefficient; a the radius of the crystal; and x the distance from the point source to the front surface of the crystal. As x is increased, the expression is rapidly asymptotic to an inverse square law where the distance is measured to the center of the crystal.

IX. EXPERIMENTAL OBSERVATIONS

The order in which the materials were studied was (a) aluminum, (b) sodium, and (c) magnesium. Since small amounts of the target materials tended to evaporate from certain targets due to the heating induced by the proton beam, and thus contaminated the target chamber and associated piping, it became necessary to exert care with regard to the types of materials introduced into the target chamber, previous to, or during a given investigation. The only contaminant possible during (a) was fluorine which had been used for calibration purposes. The fluorine gammas were observed. Hence, the presence of 6-Mev gammas in an Al+ p spectrum could at least in part be ascribed to this impurity. In (b), the possible contaminants were aluminum and fluorine. Since the previously observed Al+ p peaks were not observed to any significant extent in (b), there was no danger of falsely assigning any aluminum impurity peaks to the sodium reaction. In (c) the possibility of target chamber contamination was increased to include sodium. This contamination was observed, and it became necessary to disassemble the target chamber and clean it.

Excitation curves were run for each resonance in order to determine the yield of the reaction, detect impurities and check the voltage scale. The area under pulse-height distributions generally agreed within 10 percent with the excitation curves run with the integral discriminator. The observed yields and calculated extrapolated yields are given in Table II. The integral discriminator was generally set to count pulses greater than 1 Mev in height.

(a) Aluminum Bombarded with Protons.



Since the excitation curves obtained using ordinary aluminum indicated the presence of impurity radiations, specially purified aluminum was procured from our Institute for the Study of Metals. With this aluminum whose purity was specified as greater than 99.99 percent, only the aluminum resonances were observed. The targets were machined into disk form using a clean, sharp tool.

The two resonances which gave enough intensity for gamma analysis were located at 325 kev and 404 kev. Thick target spectra were obtained at 415 kev and in the region 335 to 350 kev. The former included both resonances; the latter only the 325-kev resonance. A 6-Mev gamma-ray appeared on both sets of curves and was attributed to fluorine contamination. The two

TABLE II. Total gamma-ray yields.

Reaction	Target	Observed thick target yield of pulses > 1 Mev (counts of 64/500 μ coul)	Total extrapolated yield ^a (counts of 64/500 μ coul)
$\text{Na}^{23} + p \rightarrow \text{Mg}^{24}$ (305-kev resonance)	Na_2SO_4	80	94
$\text{Mg}^{24} + p \rightarrow \text{Al}^{25}$ (222-kev resonance)	Magnesium (evaporated)	4.5	8
$\text{Mg}^{26} + p \rightarrow \text{Al}^{27}$ (314-kev resonance)	Magnesium (evaporated)	4	6
$\text{Mg}^{26} + p \rightarrow \text{Al}^{27}$ (336-kev resonance)	Magnesium (evaporated)	60	80
$\text{Al}^{27} + p \rightarrow \text{Si}^{28}$ (325-kev resonance)	Solid pure aluminum	7	9
$\text{Al}^{27} + p \rightarrow \text{Si}^{28}$ (404-kev resonance)	Solid pure aluminum	28	37

^a Gamma components of 0.5 Mev or less are not included.

spectra appeared to be of the same shape with all other components occurring in the same proportions. The observed peaks, their interpretation in terms of gamma-energies, and estimated intensities are given in Table III. It should be noted that the intensity values given at $E_p = 415$ kev include both resonances. If the lower voltage yields are subtracted from the upper ones, a ratio of about 5:1 is obtained for the relative intensity of the two resonances. Over a dozen runs in total were made, and average spectra are shown in Figs. 5(a) and 5(b). The pulse-height distribution for the 7-Mev gamma-rays at $E_p = 415$ kev was compared with the corresponding part of the distribution at 330 kev by alternately running over the peaks observed at these proton energies. The results were very nearly the same.

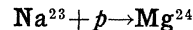
The difference in the average values listed in Table III is not believed to be significant.

Although the pulse-height analyses were not carried out beyond pulse heights of about 7.5 Mev (gamma-energies greater than 8.5 Mev), the absence of any appreciable plateau above the peaks due to the observed 7-7.5 Mev gamma-rays indicates that no higher energy gammas of comparable intensities were being emitted.

The characteristics of the spectrum may be described by dividing it into three parts: gammas of energy 1.8-2.8, 4.5-5, and 7-7.5 Mev. (The possible presence of gammas below 1 Mev was not investigated.) The interpretation of the peaks in the 1.8-2.8-Mev region was made difficult by their spacing of approximately 0.5 Mev. Although only the 1.8- and 2.8-Mev values are quoted, a 2.3-Mev gamma might be present with low intensity. In the 4.5-5-Mev region, at least two gamma-rays were present, making the identification of peaks even more difficult.

In the case of 7-7.5-Mev gamma-rays, the appearance of a distinct peak in the distribution is clearly evident. Although the presence of two components is indicated in Fig. 5 and Table III, the combination of insufficient resolving power and poor statistics do not permit this to be done with absolute certainty.

(b) Sodium Bombarded with Protons.



As investigated by Tangen,¹² the 305-kev resonance in sodium is the only relatively strong resonance in the neighborhood of, or below, 300 kev. Other possible

TABLE III. Gamma-rays from reaction $\text{Al}^{27} + p \rightarrow \text{Si}^{28} + \gamma$.

P_1 : pair peak with escape of both annihilation quanta, at $E_\gamma - 2mc^2$.

P_2 : pair peak with escape of one of the annihilation quanta, and Compton peak superimposed, at approximately $E_\gamma - mc^2$.

Resonances involved (kev)	(a) Gamma-energies			Energy of associated γ -ray (Mev)	E_γ (Mev)	(b) Gamma-intensities	
	Observed peak location (Mev)	Identification on Figs. 5(a), 5(b) and interpretation				Extrapolated yield (counts of 64/500 μ coul)	Relative intensity (counts of 64/500 μ coul)
404+325 ($E_p = 415$ kev)	1.81±0.05	B	Photo	1.81±0.05	1.81±0.05	14	12
			P_1	2.83±0.07			
	2.31±0.07	C	P_2	2.82±0.07	2.82±0.07	12	12
	2.82±0.07	D	Photo	2.82±0.07			
	3.63±0.10	E	P_1	4.65±0.10	4.65±0.10	Sum ~5	Sum ~5
	4.02±0.10	F	P_2	4.65±0.10	5.04±0.10		
			P_1	5.04±0.10			
	4.47±0.13	G	P_2	5.04±0.15			
	5.11±0.15	...	P_1	6.13±0.15	6.13±0.15	2	2
	6.10±0.15	H	P_1	7.12±0.15	7.12±0.15	Sum ~12-16	Sum ~12-16
	6.44±0.15	I	P_1	7.46±0.15	7.46±0.15		
	1.75±0.10	Interpretations same as above			1.75±0.10		2
2.73±0.13				2.73±0.13		2	2
3.66±0.14							
325	4.07±0.16			4.67±0.14		Sum ~1	Sum ~1
	5.20±0.15			5.09±0.16			
	6.14±0.18			6.22±0.15	1.7	1.7	
	6.60±0.23			7.16±0.18		Sum 2	Sum 2
			7.60±0.23				

¹² Reference 1, p. 56 ff.

resonances in this region of operating voltage are about a factor of 100, or more, lower in intensity.

The excitation curves obtained in the present work were consistent with the above, and hence any gamma-rays observed could be assigned to this resonance.

The data were obtained from about eight runs using both thick and thin targets of sodium sulfate. A spectrum obtained with sodium nitrite showed the same features as the others.

A gamma-ray in the region 10–10.5 Mev, at least one in the neighborhood of 7.5 Mev, and one at about 1.38 Mev are clearly visible. In the pulse-height region 2 to 3.5 Mev which would correspond to gamma-rays of energy 2 to 4.5 Mev, the intensity is relatively high but the peaks are poorly resolved. Since the peaks could not be interpreted with certainty in the latter region, the yield and intensity (given in Table IV) were estimated for the sum of all components present there. A typical spectrum is shown in Fig. 6.

(c) Magnesium Bombarded with Protons

The work of Tangen and others¹³ has resulted in the identification of the 290, 314, 336, and 388 keV resonances in magnesium with the reaction $Mg^{26}(p,\gamma)Al^{27}$, and the 222-keV resonance¹⁴ with the reaction $Mg^{24}(p,\gamma)Al^{25}$. In the present work, the 222, 314, and 336 keV resonances were studied. The 290-keV resonance, being just detectable on the excitation curves, was too weak to be analyzed.

The magnesium targets, both thick and thin, were prepared by evaporation in vacuum onto the copper target disks.

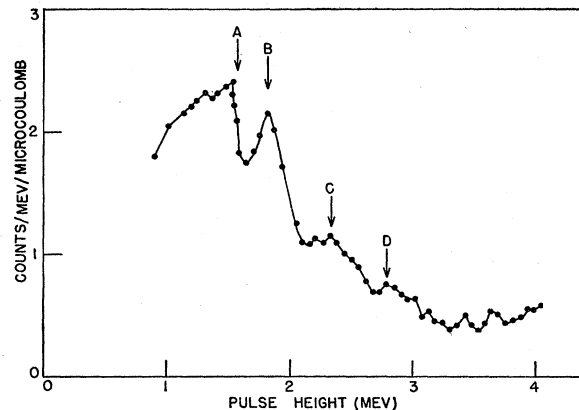
A total of nine thick target and eight thin target runs were made. Since more peaks were detectable on the higher energy thick target curves than the sum total of peaks on the thin target curves, it was concluded that small amounts of impurities were present. For this reason, the results of thin target bombardment were used to identify the gamma-ray peaks associated with the 336 and 314 keV resonances.

(1) $Mg^{24}(p,\gamma)Al^{25}$ (222 keV Resonance)

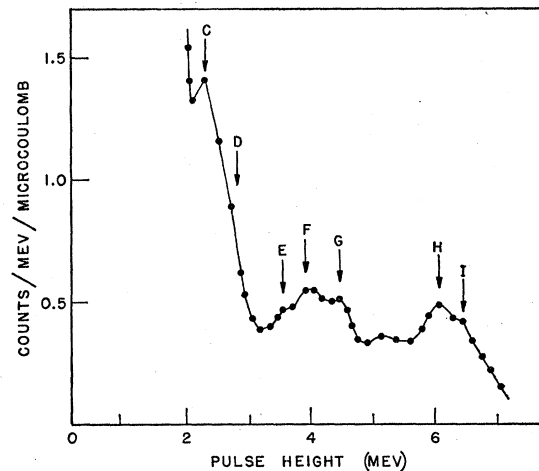
The measurements on this resonance were carried out using thick targets only. The existence of the resonance was verified by running an excitation curve with the discriminator set to count all pulses greater than 0.5 Mev in height. A sharp step appeared at 222 keV (an increase by a factor of about 4 above background). The curve then remained flat up to and above 280 keV. From this, it was concluded that resonances due to impurities were not present in this region, and since larger beam currents were obtainable at the higher proton energies, the data for this resonance were taken at 270 keV.

¹³ Reference 1, p. 58 ff.

¹⁴ Grodta, Lönsjö, and Tangen, Phys. Rev. **77**, 296 (1950).



(a)



(b)

Fig. 5. (a) $Al^{27}(p,\gamma)Si^{28}$ low energy gamma-spectrum. ($E_p = 415$ keV.) In this region, two gamma-rays are observed: a 1.8-Mev gamma-ray, with Compton edge and photopeak at A and B, respectively; and a 2.8-Mev gamma-ray, with peaks at B, C, and D. (b) $Al^{27}(p,\gamma)Si^{28}$ high energy gamma-spectrum (thick target), showing gamma-peaks above 2 Mev. Peak C is the same as peak C in Fig. 5(a); peak D of that figure is not resolved here. The presence of two gamma-rays of energy 4.65 and 5.04 Mev is determined from peaks E, F, and G. (Since two peaks are generally observed per gamma-ray in this energy region, F is considered to be an unresolved double peak.) Peaks H and I are the pair peaks (P_1) due to the 7.12 and 7.46-Mev gamma-rays (only one peak per gamma is resolved in this energy region).

Two spectra covering the pulse-height region 0.5–2.5 Mev were obtained (see Fig. 7). The absence of γ -rays above 2.5 Mev in energy was obvious in that with the integral discriminator set to count pulses above 2.5 Mev, the number of counts obtained was negligible.

The Compton distribution and photopeak of a 1.9-Mev gamma-ray appeared. There is a peak at 0.9 Mev which could be the pair peak. A smaller peak at 2.3 Mev may be interpreted as the photopeak of a 2.3-Mev gamma-ray.

A photopeak is also observed at 0.5 Mev which may be due to the annihilation of the decay positrons of Al^{25} , a nuclear γ -ray of this energy, or a combination of

TABLE IV. Gamma-rays from reaction: $\text{Na}^{23} + p \rightarrow \text{Mg}^{24}$ proton resonance at 305 kev. P_1 : pair peak with escape of both annihilation quanta, at $E_\gamma - 2mc^2$. P_2 : pair peak with escape of one of the annihilation quanta, and Compton peak superimposed, at approximately $E_\gamma - mc^2$.

Observed peak location	(a) Gamma-ray energies			(b) Gamma-ray intensities	
	Identification in Fig. 6, and probable interpretation	Energy of associated γ -ray	E_γ	Extrapolated yield (counts of 64/500 μcoul)	Relative intensity (counts of 64/500 μcoul)
1.00 ± 0.03	—	Compton	1.38		
1.38 ± 0.04	A	Photo	1.38	1.38 ± 0.04	28
		P_1	2.40	(?) 1.90 ± 0.11	
		Photo	1.90		
1.90 ± 0.11	B	P_2	2.4		Sum ≤ 5
		P_1	2.92		Sum ≤ 4
		Photo	2.41	2.41	
2.41 ± 0.12	C	P_2	2.9		
		P_1	3.43		
		Photo	2.88	2.88	
2.88 ± 0.14	D	P_2	3.4	3.4	
		P_1	3.90	3.9	Sum ≈ 24
3.22 ± 0.13	E	P_2	3.7	3.7	Sum ≈ 24
		P_1	4.24		
3.65 ± 0.14	—	P_2	4.2	4.2	
		P_1	4.67		
4.74 ± 0.14	—	P_1	5.76	$5.76 - 0.14$	≤ 5
5.13 ± 0.15	—	P_1	6.15	$6.15 - 0.15$	≤ 2
5.82 ± 0.24	F	P_1	6.84	$6.84 - 0.24$	Sum ≈ 20
6.48 ± 0.20	G	P_1	7.50	$7.50 - 0.20$	Sum ≈ 20
9.3 ± 0.3	H	P_1	10.3	$10.3 - 0.3$	12

both. The spectrum interpretation and yield estimates are given in Table V.

(2) $\text{Mg}^{26}(p,\gamma)\text{Al}^{27}$ (336-kev Resonance)

The presence of only two gamma-rays was discernible from the thin target curves: a 5.8-Mev and a 2.8-Mev gamma-ray (see Fig. 8). The intensities of the two gamma-rays were comparable. The observed yield for the 2.8-Mev gamma-ray, as given in Table VI was lower than for the 5.8-Mev gamma-ray. However, since the thin magnesium targets were difficult to work with, having a tendency to evaporate under bombardment, these relative yield figures are probably not very reliable.

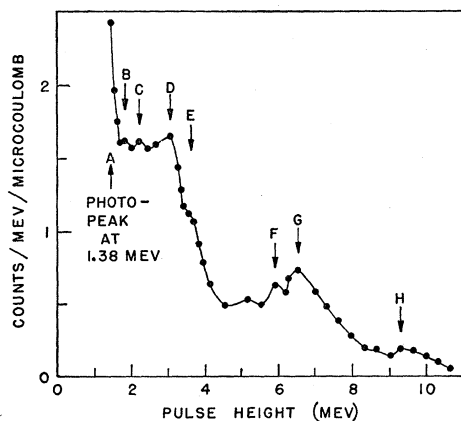


FIG. 6. $\text{Na}^{23}(p,\gamma)\text{Mg}^{24}$ gamma-ray spectrum (305-kev resonance). Peaks B, C, D, and E are not sufficiently well resolved to permit certain identification of the gamma-rays involved. Peaks F, G, and H are the pair peaks (P_1) due to the 6.8-, 7.5-, and 10.3-Mev gamma-rays, respectively.

(3) $\text{Mg}^{26}(p,\gamma)\text{Al}^{27}$ (314-kev resonance)

This resonance is about 1/12 as strong as the 336-kev resonance. The observed thin target yield above 1 Mev was about twice background. Because of very poor statistics in this case (this being the weakest of all the resonances analyzed), the interpretation of the observed spectrum is somewhat in doubt. The information about the spectrum was obtained from one thick target and two thin target curves.

To make sure that the observed pulse-height distributions were actually due to this resonance, the areas under the thin target curves were calculated. The results were compared with the yield at 314 kev obtained from the excitation curves and were essentially the same.

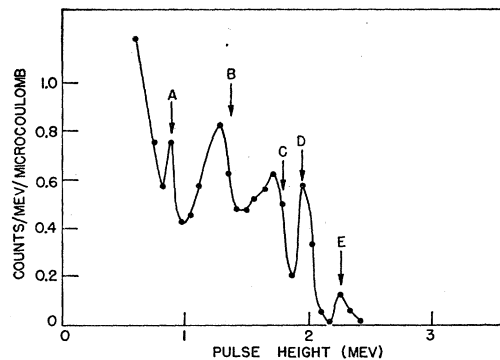


FIG. 7. $\text{Mg}^{24}(p,\gamma)\text{Al}^{25}$ gamma-spectrum due to the resonance at a proton energy of 222 kev. Thick target; $E_p = 270$ kev; 500 microcoulombs per point. Peak D is interpreted as the photopeak of a 1.95-Mev gamma-ray, with pair peak (P_1) at A and Compton edge at C; peak E, the photopeak of a 2.3-Mev gamma, with pair peak (P_1) at B.

TABLE V. Gamma-rays from reaction: $Mg^{24} + p \rightarrow Al^{25} + h\nu$.

P_1 : pair peak with escape of both annihilation quanta, at $E_\gamma - 2mc^2$.

P_2 : pair peak with escape of one of the annihilation quanta, and Compton peak superimposed, at approximately $E_\gamma - mc^2$.

Resonance energy (keV)	Observed peak location (Mev)	Identification in Fig. 7 and interpretation	Energy of associated γ -ray (Mev)	Extrapolated yield (counts of 64/500 μ coul)	Relative intensity (counts of 64/500 μ coul)
222	0.48 \pm 0.05	...	0.48 \pm 0.05	30	\sim 6 (nuclear component)
	0.94 \pm 0.05	A			
	1.60 \pm 0.06	C	Compton photo	6	6
	1.94 \pm 0.06	D			
	1.30 \pm 0.05	B	P_1 photo	2.35 \pm 0.1	2
	2.35 \pm 0.1	E			

As a further check, the 314-keV and 336-keV resonance yields were calculated, giving a ratio of about 1/14. From the data obtained by Tangen, who used G-M counter detection, a ratio of about 1/12 was estimated for the two resonance yields, which would seem to be a satisfactory agreement. The location of the resonance also agreed with his value (314) within 1 kilovolt.

In spite of the low yield, it is concluded that the 5.8-MeV gamma-ray which predominated at the 336 keV resonance did *not* appear at 314 keV. Instead, the observed increased counting rates were observed in the region of 3 to 3.5 MeV pulses, corresponding to one or more gamma-rays in the neighborhood of 4 MeV in energy.

X. DISCUSSION AND CONCLUSIONS

The "relative intensity" numbers listed in Tables III-VI (definition given in Sec. VIII) are proportional to the number of quanta of each energy which would have been absorbed in the crystal if the efficiency of the crystal had been a constant, independent of gamma-energy. Assuming that differences in the angular distributions of the emitted gamma-rays are not important (in view of the large solid angle accepted by the crystal, and the rather broad target), the "relative intensity" numbers are then proportional to the number of quanta of each gamma-energy emitted from the target per incident proton.

(1) $Al(p,\gamma)Si^{28}$

At the 325- and 404-keV resonances in aluminum, excited states of Si^{28} are produced having excitation energies of approximately 12.00 and 12.08 MeV, respectively,¹⁵ in the center-of-mass system.

In the absence of any competing reactions, the full energy, which is about the same in the laboratory system, must be released by the emission of gamma-rays,

¹⁵ D. E. Alburger and E. M. Hafner, Revs. Modern Phys. 22, 376 (1950).

either directly to the ground state, or in cascade, via intermediate levels.

The observed gamma-rays, 1.81 \pm 0.04, 2.82 \pm 0.07, 4.65 \pm 0.10, 5.04 \pm 0.10, 7.12 \pm 0.15, and 7.46 \pm 0.15 MeV, can be accounted for in a decay scheme (the same for both resonances) involving levels in Si^{28} at 1.81 \pm 0.05, 4.63 \pm 0.10, and 7.12 \pm 0.15 MeV. If the 7.12-MeV gamma is emitted first, and the present work cannot rule out this possibility, then an additional level, at 5.04 \pm 0.10, is involved. The "relative intensities" given in Table III for a proton energy of 415 keV (including both the 325 and 404 keV resonances), are the same for the 1.81 and 2.82-MeV gammas, each having the value 12, indicating that they may be in cascade; the sum of the intensities of the 4.65- and 5.04-MeV gammas is about 5; and the sum of the intensities of the 7.12- and 7.46-MeV gammas is between 12 and 16. These observed "relative intensities" are seen to be consistent

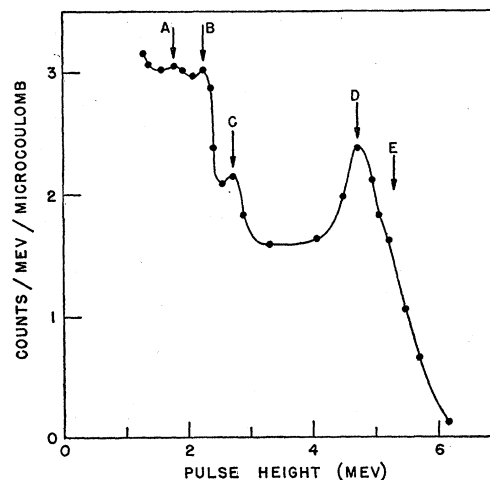


FIG. 8. Thin target gamma-spectrum from $Mg^{26}(p,\gamma)Al^{27}$ at the 336-keV resonance. $E_p=336$ keV. Peaks A, B, and C are associated with a single gamma-ray of energy 2.8 MeV. Peak D is the pair peak (P_1) due to a 5.8-MeV gamma-ray whose second peak (P_2) at E is not resolved.

TABLE VI. Gamma-rays from reaction: $Mg^{26} + p \rightarrow Al^{27} + \gamma$. P_1 : pair peak with escape of both annihilation quanta, at $E_\gamma - 2mc^2$. P_2 : pair peak with escape of one of the annihilation quanta, and Compton peak superimposed, at approximately $E_\gamma - mc^2$.

Resonance energy (kev)	Observed peak location (Mev)	Identification in Fig. 8 and interpretation		Energy of associated γ -ray (Mev)	Extrapolated yield (counts of 64/500 μ coul)	Relative intensity (counts of 64/500 μ coul)
336	1.85 ± 0.10	A	P_1	2.83 ± 0.14	35	35
	2.25 ± 0.12	B	P_2			
	2.83 ± 0.14	C	Photo			
	4.78 ± 0.25	D	P_1	5.80 ± 0.25	45	45
5.30 ± 0.25	E	P_2				
314	(?) 3.20 ± 0.2	—	P_1	(?) 4.2 ± 0.2	3	3
	(?) 3.70 ± 0.2	—	P_2			

with the requirements of the proposed decay scheme, which is drawn in Fig. 9.

Levels in Si^{28} at 1.78 ± 0.13 , 4.47 ± 0.10 , 4.91 ± 0.21 , and 7.10 ± 0.12 Mev have been determined by Peck¹⁶ from the neutrons emitted in the reaction $Al^{27}(d,n)Si^{28}$. These levels are seen to be consistent with the ones proposed for the decay scheme.

Rutherglen *et al.*,¹⁷ bombarding thick targets of aluminum with 750-kev protons, observed the gamma-rays with a pair spectrometer. Their bombardment included at least eight resonances between 404 kev and 750 kev in addition to the 404-kev and 325-kev resonances involved in this work. They were able to resolve three gamma-rays of energies 7.62 ± 0.1 , 10.46 ± 0.07 , and 12.12 ± 0.1 Mev, but suggested the possibility of other gamma-rays in the neighborhood of 7.6 Mev. The 7.62 ± 0.1 Mev gamma-ray is possibly the same as the 7.46 ± 0.15 Mev gamma-ray observed in the present work.

Since no gamma-energies greater than 7.5 Mev were observed for the 415-kev proton bombardments, whereas at 750 kev, 10 to 12-Mev gammas are present, it is evident that other modes of decay of the excited states of Si^{28} must be more probable in the higher resonances. According to Tangen, the mean gamma-ray energy at the 503-kev resonance (which is about six times more intense than the 404-kev resonance) is 9.2 Mev compared with 5.4 Mev at both the 404- and 325-kev resonances.

It should be mentioned that decay through a level in the neighborhood of 6.1 Mev has not been entirely excluded. Since there was known to be a small amount of fluorine contamination present, however, the observed gamma-ray of this energy was assigned to the reaction $F^{19}(p; \alpha, \gamma)O^{16}$.

(2) $Na^{23}(p, \gamma)Mg^{24}$

The excited state of Mg^{24} produced here has 12.0₃ Mev of energy, about the same as the previously discussed Si^{28} . The observed gamma-rays: 1.38 ± 0.04 Mev ("relative intensity" 28); 6.84 ± 0.24 and 7.50 ± 0.20

Mev (sum of intensities 20); 10.3 ± 0.3 Mev (intensity 11); a probable gamma-ray at 3.6 ± 0.2 Mev; and others in the region 2–4.5 Mev *do not* appear to be sufficient to determine a complete decay scheme, which is consistent with the observed relative intensities. The intensity of the 1.38-Mev gamma-ray seems to be too large to be accounted for entirely by the simple cascade:

$$(10.3 \pm 0.3) + (1.38 \pm 0.04) = 11.7 \pm 0.3.$$

Possible emission of the 7.50 ± 0.20 Mev gamma-ray to the well-known 4.14-Mev level in Mg^{24} (the 4.14 level decays by emission of a 2.76-Mev gamma to a level at 1.38 Mev) seems to be somewhat outside the limits of experimental error as far as the energy is concerned.

Since the intensity of the 1.38-Mev gamma is of the order of the sum of the intensities of the 6.84 ± 0.24 , 7.50 ± 0.20 , and 10.3 ± 0.3 gammas, it seems likely that each of these high energy gammas is part of a cascade passing through the 1.38-Mev level. Energy considerations suggest the presence of at least one gamma-ray of energy less than or equal to 0.5 Mev.

One possible decay scheme which is consistent with the experimental data would require levels at 5.1, 4.6, 1.8, and 1.38 Mev. The gamma-rays in this scheme would be 10.3, 7.4, 6.9, 3.7, 3.2, and 0.4 Mev.

(3) $Mg^{26}(p, \gamma)Al^{27}$

The excited state of Al^{27} produced at the 336-kev resonance appears to decay by means of two gamma-rays: 5.8 and 2.8 Mev. The excitation energy, as given in the paper of Alburger and Hafner, is 8.61 Mev. Energy levels at both 5.8 and 2.8 Mev are both known from other researches.¹⁸ Hence, the decay with either order of emission is shown in the decay scheme proposed in Fig. 9.

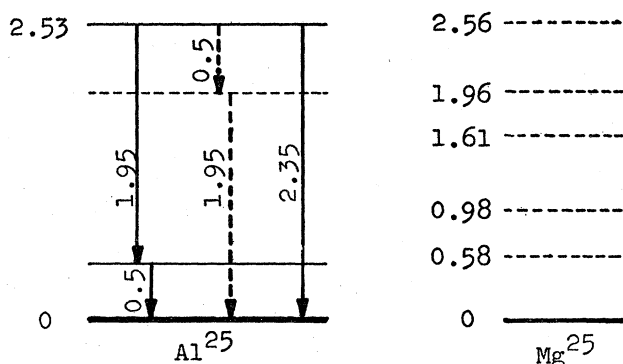
The 314-kev resonance, producing Al^{27} with approximately the same excitation energy of 8.6 Mev, showed no evidence of a 5.8-Mev gamma-ray. Low intensity prevented an extended search of the pulse-height distribution, but gamma-rays in the region of 4 Mev were indicated. It is suggested that the decay takes place

¹⁶ R. A. Peck, Phys. Rev. **76**, 1279 (1949).

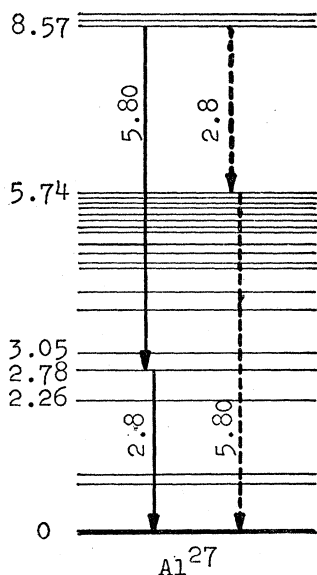
¹⁷ Rutherglen, Rae, and Smith, Proc. Phys. Soc. (London) **64**, 913 (1951).

¹⁸ For data on Al^{27} levels, see H. F. Stoddard and H. E. Gove, Phys. Rev. **87**, 238, 262 (1952); Reilly, Allen, Arthur, Bender, Ely, and Hausman, Phys. Rev. **86**, 857 (1952).

(a) $Mg^{24} + p ; E_p = 222 \text{ kev}$



(b) $Mg^{26} + p ; E_p = 336 \text{ kev}$



(c) $Al^{27} + p ; E_p = 325, 404 \text{ kev}$

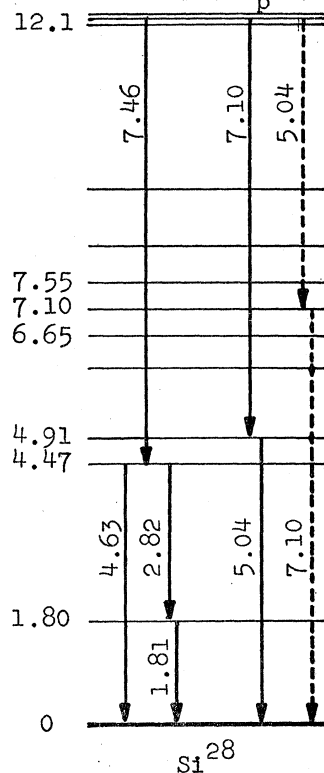


FIG. 9. Energy level diagrams drawn for Al^{26} , Al^{27} , and Si^{28} with level positions obtained from the literature. The gamma-transitions indicated are the probable modes of decay from the excited states, as determined from the observed gamma-rays. A permutation of the order of emission of 2 gammas, which is also consistent with the experimental results and a known intermediate level, is indicated by dashed lines. The known levels of Mg^{26} are drawn in dashed lines for comparison with the present results for the mirror nucleus Al^{26} .

either through a 4.3-Mev (known) level with emission of two 4.3-Mev gammas, or through some other level in the neighborhood of 4 Mev of excitation energy.

(4) $Mg^{24}(p,\gamma)Al^{25}$

The observed gamma-rays 1.95 ± 0.06 Mev (intensity 6), 0.48 ± 0.05 Mev (intensity 6), and 2.35 ± 0.1 Mev

(intensity 2) can be combined into the decay scheme shown in Fig. 9. This scheme is in reasonable agreement with an estimated excitation energy of $2.3 + 0.21 = 2.5$ Mev, where 2.3 Mev is the estimated¹⁹ binding energy of a proton added to Mg^{24} , and 0.21 Mev is the kinetic

¹⁹ See, for example, Louis T. Koester, Phys. Rev. 85, 643 (1952).

TABLE VII. Estimated yields.

Reaction	Proton energy at resonance (kev)	Target	Estimated number of reactions per proton $\times 10^{12}$
$\text{Na}^{23}(p,\gamma)\text{Mg}^{24}$	305	Thick Na_2SO_4	19
$\text{Mg}^{24}(p,\gamma)\text{Al}^{25}$	222	Thick magnesium	5.0
$\text{Mg}^{26}(p,\gamma)\text{Al}^{27}$	314	Thick magnesium	1.9
	336	Thick magnesium	25
$\text{Al}^{27}(p,\gamma)\text{Si}^{28}$	325	Thick aluminum	1.3
	404	Thick aluminum	7.5

energy of a proton in the center-of-mass system for the 222-kev resonance. It should be noted that the presence of 0.9- and 1.6-Mev gamma-rays, whose energies would also add up to the estimated excitation energy, cannot be excluded, as may be seen from Table IV. Support for the above results may be obtained by comparison with the energy levels of the mirror nucleus Mg^{25} as given by Endt *et al.*²⁰ They give 0.583, 0.976, 1.611, 1.957, and 2.562 Mev for the first five excited states.

On the basis of the proposed decay schemes, the relative intensities, and the geometry of the detecting

²⁰ Endt, Enge, Haffner, and Buechner, Phys. Rev. 87, 27 (1952).

system, it becomes possible to estimate the reaction probabilities, i.e., the number of (p,γ) reactions taking place per proton hitting each of the thick targets. In the case of the sodium reaction, even without a complete decay scheme, it seems reasonable to assume that the 10.3, 7.5, and 6.8 Mev gammas are the members of three distinct cascades which are the principle ones that occur. Adding the relative intensities of the primary γ -rays of the various modes of decay gives the total relative probability that the (p,γ) reaction takes place.

Using Eqs. (2) and (3) and a distance of about 0.8 in. between target and the center of the crystal, with 0.135 in. of copper in between, an over-all detection efficiency at 6 Mev of about 3.2 percent is obtained.

The resultant calculated reaction probabilities are given in Table VII. They are believed to be correct within about a factor of 2. It may be noted that the most probable of these reactions is less probable by a factor of about 10^3 than the fluorine reaction at 340 kev in CaF_2 . The latter is given in the literature as 1.7×10^{-8} .

I wish to express my gratitude to Professor Samuel K. Allison, in whose laboratory this work was done, for suggesting that the problem be undertaken, and for giving invaluable assistance and guidance whenever it was most needed. Thanks are due Gordon duFloth, Peter K. Weyl, and Elias Snitzer for their help with operational problems of the kevatron, and special thanks to Mrs. Sophie Casson who spent many evenings assisting in the taking of data, checking calculations, and helping in the preparation of this paper.